Effects of changes in vegetation on precipitation in the northern Tianshan Mountains evaluated using multiple time scales

Qinming Sun[1], Tong Liu[1,*], Zhiquan Han[2], Yongping Wu[3] and Bai-Lian Li[4]

[1]*College of Life Science, Shihezi University, Shihezi 832000, Xinjiang, China.*
[2]*Teachers College, Shihezi University, Shihezi 832000, Xinjiang, China.*
[3]*College of Physical Science and Technology, Yangzhou University, Yangzhou 225000, Jiangsu, China.*
[4]*C. XiIEG-UCR International Center for Arid Land Ecology, University of California Riverside, CA 92521-0124, USA.*
[*]*Corresponding author. e-mail: betula@126.com*

This study used a combination of the wavelet cross-correlation technique and numerical analysis of vegetative feedback to study the role of climate–vegetation feedback from 1981 to 2009 in the northern Tianshan Mountains, Xinjiang Province, China. The study area included the Irtysh River, the Bortala and Ili River valleys, the northern slopes of the Tianshan Mountains, and the western Junggar Basin. The feedback effects of changes in vegetation on precipitation appeared to vary in these five regions when different time scales are used to examine them. The most useful time scale was generally found to be 4–6 months. Time lag was another characteristic of this process, and the optimal time lag was 3–4 months. Nevertheless, optimal time scale and time lag did not differ significantly in these five regions. In this way, the correct time scale of the effects of variations in vegetation on precipitation in this cold, arid area was found. This time scale and time lag can be assessed through wavelet cross-correlation analysis. Then numerical analysis can be used to improve the accuracy of the analysis.

1. Introduction

A correlation exists between climate and vegetation on regional and even global scales, where climate controls the spatial distribution of types of vegetation. However, vegetation can affect climate by affecting air exchange in the atmosphere (Brovkin *et al.* 2006; Davin and De Noblet-Ducoudré 2010; Zhang *et al.* 2013). In the current study, climatological models were used to evaluate the interactions between climate and vegetation. One of the limitations of such models is that the ideal time scale for the evaluation of this relationship has not yet been identified (Zeng 2003; Paeth *et al.* 2009; Pitman *et al.* 2009; Alo and Wang 2010; Wu *et al.* 2011). The simplification of traditional dynamics and theoretical analysis rarely involves analysis of the time scales of climate–vegetation feedback when they deal with the relationship between vegetation and atmosphere. However, identifying the response time of changes in climate and vegetation is very important. This assessment may provide an observational benchmark that can be tested by coupled global vegetation–climate models. They will be very important in providing further understanding of and better insight into the mechanisms

Keywords. Northern Tianshan Mountains; relationship between vegetation and precipitation; time lag; wavelet cross-correlation analysis.

of climate–vegetation feedback and the possible effects of the land use changes in current regional climate changes.

In recent years, remote sensing technology has continued to develop; this permits scholars to use long-term observational data related to vegetation indices and climate to study the relationships between climate and changes in vegetation on different spatial scales (Zhang *et al.* 2003; Liu *et al.* 2006; Hua *et al.* 2008; Mao *et al.* 2008; Wang *et al.* 2010; Zuo *et al.* 2010; Wu *et al.* 2011). Studies in many parts of the world have shown that vegetation changes have a positive feedback relationship with average monthly temperature, monthly maximum temperature, and the degree of variation in average monthly temperature (Wu *et al.* 2011). On an inter-annual time scale, Liu *et al.* (2006) and Li *et al.* (2008) demonstrated that the positive feedback effect that changes in vegetation on precipitation is very pronounced in northeastern Brazil, eastern Africa, eastern Asia, and northern Australia. On a seasonal scale, changes in vegetation cover have some negative feedback effects on the frequency of light rain and on the onset of the late period in agriculture in the ecotones and grasslands of northern China (Mao *et al.* 2008). The normalized difference vegetation index (NDVI) in winter has a distinctly positive correlation with the amount of precipitation that falls on the Tibetan Plateau and in central China during the following summer. The spring NDVI also has a correlation with the amount of precipitation that falls on the Tibetan Plateau and in the arid and semi-arid regions in the eastern part of northwestern China during the following summer (Zhang *et al.* 2003; Hua *et al.* 2008). The research discussed above was usually conducted using monthly and seasonal time scales for cross-correlation analysis under different time delay conditions, but the changes in vegetation and climate showed multiple time scale characteristics. For this reason, revealing feedback effects of changes in vegetation as they are related to precipitation has proved helpful. This can be done by studying the correlations between NDVI and changes in precipitation using different time scales and different regional conditions.

The numerical simulation calculation method is a common means of studying the inter-relationships and feedback between climate and vegetation. This method has been shown to be very precise in studies of climate–vegetation feedback (Liu *et al.* 2006; Notaro and Liu 2008). However, the method focusses on the feedback inter-relationships between climate and vegetation at a single time scale, selects a single analysis scale, and ignores time lag. Therefore, it cannot fully reflect the effects of feedback on changes in vegetation on precipitation, if those effects have multiple times-cale characteristics.

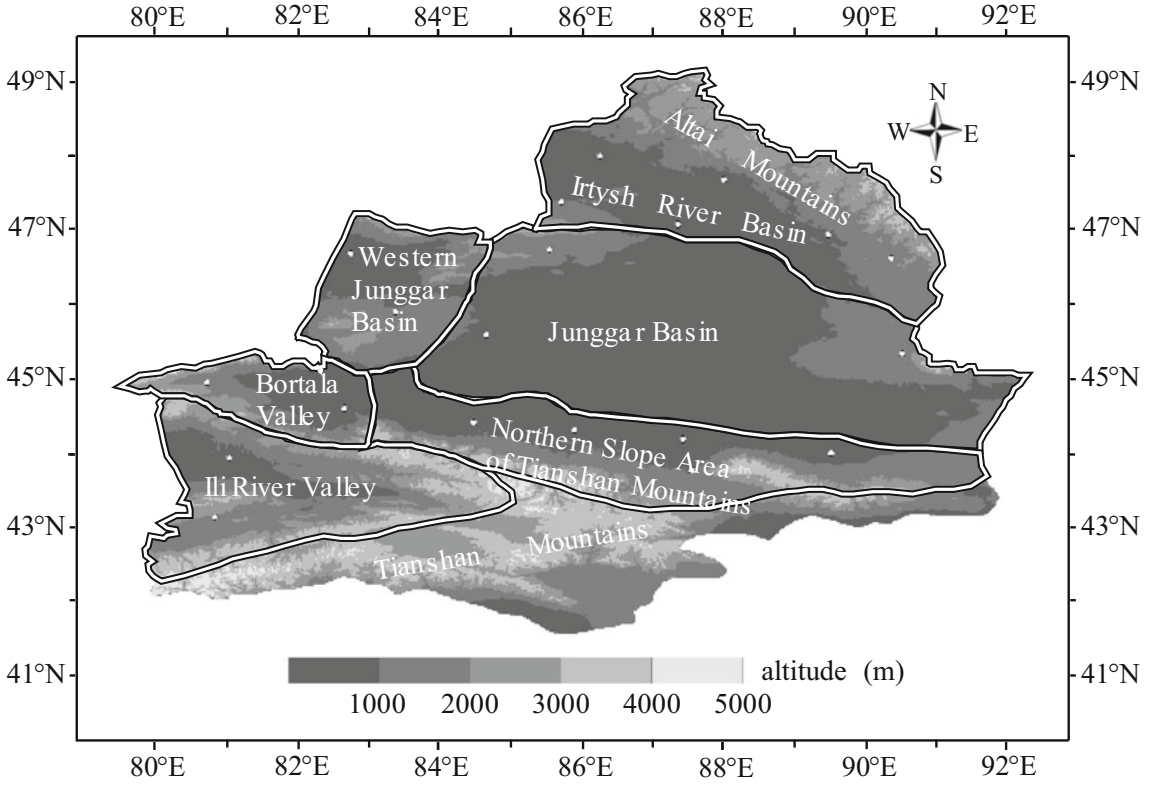

Figure 1. Location of the northern Tianshan Mountains, Xinjiang, China. The white dots indicate meteorological data collection sites.

The northern Tianshan Mountains are located in Xinjiang Province, which includes the Irtysh River Basin, the Bortala valley, Ili River valley, the Junggar Basin, the northern slopes of the Tianshan Mountains, and the mountains in the western part of the Junggar Basin. The region lies far from the ocean and is surrounded on three sides by the Tianshan, Tarbagatai, and Altai mountains (figure 1). This basin allows the formation of a unique local climate system providing an ideal environment for the study of regional climate–vegetation interactions (Zhang and Deng 1987; Zhang 2001; Shi *et al.* 2002).

The wavelet analysis (WA) method can be used to perform integrated analysis of non-stationary time series, making it applicable to studies of complex systems that vary across multiple time scales (Li 2000; Wang *et al.* 2009). Methods based on wavelet cross-correlation analysis can facilitate quantitative descriptions of the relationships between two non-stationary time series for specific time scales and time lags. This has advantage over ordinary relative analysis and cross-spectral analysis, allowing it to be used to determine cross-correlations of vegetation and climate on multiple time scales. In recent years, the WA method has been widely used in studies of climate change (Paluš *et al.* 2005; Rehman and Siddiqi 2009; Brunsell 2010) and to analyse changes in hydrology and water resources as well as changes in vegetation (Gao and Li 1993; Li and Loehle 1995; Xie and Liu 2010; Hudson *et al.* 2011; Kisi 2011; Wang *et al.* 2011). However, WA has seldom been used in studies of vegetation–climate relationships.

In the present study, numerical analysis of feedback information from vegetation, combining WA and cross-correlation techniques, was used to study the feedback effect of the changes in vegetation on precipitation on different time scales and time lags. It was also used to study the characteristics of the effects of changes in vegetation on precipitation over a 30-year period (1981–2009) in the northern Tianshan Mountains, Xinjiang Province, China. Then, the feedback relationship between changes in vegetation and precipitation over time was summarized. These results may improve on use of the numerical analysis method in the analysis of the feedback effects of changes in vegetation.

2. Methods

2.1 *Data pre-processing*

The Junggar Basin region covers a large area with only three meteorological stations. Precipitation is a spatially noisy climate variable, an average of precipitation from the three meteorological stations would probably not be representative of the entire Junggar region. In this region, vegetation was sparse, and the feedback effects on precipitation were weak. Therefore, this research focussed on five regions: (1) the Irtysh River Basin, (2) the Bortala valley, (3) the Ili River valley, (4) the northern slopes of the Tianshan Mountains, and (5) the mountains in the western part of the Junggar Basin (figure 1). We selected 18 of the available weather stations and evaluated daily meteorological data from January 1, 1981 to December 31, 2009 to guarantee the uniformity and stability of the meteorological data analysed. The National Meteorological Information Center of the China Meteorological Administration (http://www.nmic.gov.cn/) provided meteorological data.

Satellite data used here consisted of NOAA/Advanced Very High Resolution Radiometer (AVHRR) NDVI digital images (1981–2001) provided by the Environmental and Ecological Science Data Center for Western China (http://westdc.westgis.ac.cn, at a spatial resolution of 1 km×1 km and at a 10-day interval) and SPOT-4 VEGETATION NDVI digital images (1998–2010) provided by VITO in Belgium (http://free.vgt.vito.be, at a spatial resolution of 1 km × 1 km and at a 10-day interval). The processing techniques addressed radiometric calibration, geometric corrections, the reduction of the effects of variable cloud cover, and recalibration during the data preparation phase. NDVI composites were created using the maximum value composite (MVC) technique, which select the highest NDVI at each pixel from daily images taken over a period of 10 days to minimize the effect of cloud cover. To assure that high quality data were used, we employed only datasets that had already seen widespread use in the study of global and regional changes in vegetation (Goetz *et al.* 2006; Kaptué Tchuenté *et al.* 2011). International general MVC were used to calculate the NDVI values on different time scales (Stow *et al.* 2007). This approach is based on the logic that low-value observations are either erroneous or have less vegetation vigor for the period under consideration (Holben 1986).

Because the data from NOAA/AVHRR and SPOT-4 involved two different sensors, we confirmed the consistency of the data and found the correlation coefficient of these two types of data to be 0.932 which exceeded the selected confidence level ($p < 0.05$), indicating a high level of data consistency (Zhang *et al.* 2011).

The analysis of the relationships between NDVI and precipitation was performed based on regions. The precipitation series was formed by averaging stations data in all regions. The NDVI data for each meteorological stations were extracted from

the mean of 5 × 5 pixels around the location of the stations, according to the geographical position, using ArcGIS. The NDVI series was formed by averaging station NDVI data in all regions. The time resolution of NDVI and precipitation were both 10 days. The 10-day anomalies of both NDVI and precipitation were further calculated as the departures from their climatological annual cycles. Finally, the data were linearly de-trended.

2.2 *Mann–Kendall (MK) test for trend*

The Mann–Kendall (Mann 1945; Kendall 1975) test is a non-parametric trend analysis for identifying the increasing and decreasing pattern in time series of the data. Non-parametric test treatment methods are based on low-precision data, so that they can handle almost any types of data. Mann–Kendall method is a non-parametric statistical test.

For a time series $X = \{x_1, x_2, \ldots, x_n\}$, in which $n > 10$, the standard normal statistic Z is estimated as:

$$Z_c = \begin{cases} \dfrac{S-1}{\sqrt{\mathrm{var}\,(S)}}, & S > 0 \\ 0, & S = 0 \\ \dfrac{S+1}{\sqrt{\mathrm{var}\,(S)}}, & S < 0 \end{cases} \tag{1}$$

where

$$S = \sum_{i=1}^{n-1} \sum_{k=i+1}^{n} \mathrm{sgn}(x_k - x_i)$$

$$\mathrm{sgn}(\theta) = \begin{cases} 1, & \theta > 0 \\ 0, & \theta = 0 \\ -1, & \theta < 0 \end{cases}$$

$$\mathrm{var}[S] = \frac{[n(n-1)(2n+5) - \sum_t t(t-1)(2t+5)]}{18} \tag{2}$$

The presence of statistically significant trend is evaluated using the Z value. At a 5% significance level, the null hypothesis of no trend is rejected if $|Z| \triangleright 1.96$. A positive value of Z denotes an increasing trend, and the opposite corresponds to a decreasing trend.

The MK non-parametric test is widely applied for determining the occurrence of abrupt change points of meteorological and hydrologic series. Advantage of the method is not only simple calculation but also confirmation of the starting time of abrupt changes and identification of the area of abrupt changes. Let $x_1, x_2, \ldots, x_n$ be the data points. For each element x_i, the numbers r_i of elements x_j preceding it $(j < i)$ such that $x_j < x_i$ are computed. Under the null hypothesis (no abrupt change point), the normally distributed statistic S_k can be calculated via the following formula:

$$S_k = \sum_{j=1}^{k} r_i, \quad 2 \le k \le n. \tag{3}$$

Mean and variance of the normally distributed statistic S_k can be given by the following formula:

$$S = E\,(S_k) = \frac{k\,(k-1)}{4},$$

$$\mathrm{var}(S_k) = \frac{k\,(k-1)\,(2k+5)}{72}. \tag{4}$$

The normalized variable statistic UF_k is estimated as follows:

$$UF_k = (S_k - S)\,\sqrt{\mathrm{var}(S_k)} \tag{5}$$

The normalized variable statistic UF_k is the forward sequence, and the backward sequence UB_k is calculated using the same equation but with a reversed series of data. When the null hypothesis is rejected (i.e., if any of the points in the forward sequence is outside the confidence interval), the detection of an increasing ($UF_k > 0$) or a decreasing ($UF_k < 0$) trend is indicated. The sequential version of the test used here enables detection of the approximate time of occurrence of the trend by locating the intersection of the forward and backward curves of the test statistic. If any intersection appears in the confidence interval, it indicates an abrupt change point.

2.3 *Wavelet cross-correlation analysis*

The traditional cross-correlation coefficient r, which is a measure of linear association between two variables, is defined as:

$$r = \frac{\sum_{i=1}^{n} \left(x_i - \overline{X}\right)\left(y_i - \overline{Y}\right)}{\sqrt{\sum_{i=1}^{n} \left(x_i - \overline{x}\right)^2 \left(y_i - \overline{y}\right)^2}}. \tag{6}$$

The traditional cross-correlation analysis is not very useful for analysing non-stationary series because it fails to describe the frequency content of a series at a particular time.

The WA method can be used to perform integrated analysis of non-stationary time series. A wavelet is a basis function characterized by two aspects. One is its shape and amplitude, which is chosen by the user. The other one is its scale (frequency) and time (location) relative to the signal. Continuous wavelet transform (CWT) can be used to generate spectrograms which show the frequency content of signals as a function of time. A continuous-time wavelet transform of $x(t)$ is defined as:

$$\mathrm{CWT}\ X_\Psi = \frac{1}{\sqrt{|a|}} \int_{-\infty}^{\infty} x\,(t) \Psi^* \left(\frac{t-b}{a}\right) dt,$$
$$\{a,\ b \in R,\ a \neq 0\}\,. \tag{7}$$

In the above equation, $\Psi(t)$ is a continuous function in the time domain as well as the frequency domain called the mother wavelet and $\Psi^*(t)$ indicates the complex conjugate of the analysing wavelet $\Psi(t)$. The parameter 'a' is termed as the scaling parameter and 'b' is the translation parameter. The transformed signal $X\Psi(a,\ b)$ is a function of the translation parameter 'b' and the scale parameter 'a'. In wavelet transform (WT), signal energy is normalized by dividing the wavelet coefficients by $|a|^{-1/2}$ at each scale.

The Morlet wavelet transform belongs to the CWT family. It is one of the most popular wavelets used in practice and its mother wavelet is given by:

$$\Psi(t) = \frac{1}{\sqrt[4]{\pi}}\left(e^{j\ w_0 t} - e^{-(w_0^2/2)}\right) e^{-(t^2/2)} \qquad (8)$$

In the above equation, w_0 refers to the central frequency of the mother wavelet. The term $e^{-(w_0^2/2)}$ involved in the above equation is specifically used for correcting the non-zero mean of the complex sinusoid, and in most cases, it can be negligible when $w_0 > 5$. Therefore, when the central frequency $w_0 > 5$, the mother wavelet is redefined as follows:

$$\Psi(t) = \frac{1}{\sqrt[4]{\pi}} e^{j\ w_0 t} e^{-(t^2/2)}. \qquad (9)$$

Methods based on wavelet cross-correlation analysis can facilitate quantitative descriptions of the relationships between two non-stationary time series for specific time scales and time lags.

Wavelet cross-correlation analysis (WCCA) is developed from the wavelet transforms and traditional cross-correlation analysis. The wavelet cross-covariance was defined as $WC_{x,y}(a,\ k)$, and the Morlet wavelet function was used to perform the wavelet transform (Sang *et al.* 2010). The continuous wavelet transform coefficient was found to have two important variables, a real variable and a module variable (Wang *et al.* 2011) as shown in equations (10) and (11), respectively:

$$WC_{xy}(a,k) = \sqrt{R(W\mathrm{cov}_{xy}(a,k))^2 + I(W\mathrm{cov}_{xy}(a,k))^2}, \qquad (10)$$

$$W\mathrm{cov}_{xy}(a,k) = E\left[W_x(a,b)\, W_y(a,b+k)\right], \qquad (11)$$

where $W_x(a,b)$ and $W_y(a,b)$ are continuous wavelet transform coefficients of the time series $x(t)$ and $y(t)$, respectively. For the scale a, k is the time lag; $R(\,)$ is the real part and $I(\,)$ is the imaginary part of the variables in parentheses; $E[\ ]$ is the mean of results in square brackets; and $WC_{xy}(a,\ k)$ is the wavelet cross-covariance of the sequence $x(t)$ and $y(t)$ in time scale (a) and time lag (k).

We then analysed the wavelet cross-correlation of the time series $x(t)$ and $y(t)$ for definition of the corresponding wavelet cross-correlation coefficient $WR_{xy}(a,\ k)$ using equation (12):

$$WC_{xy}(a,k) = \sqrt{R(W\mathrm{cov}_{xy}(a,k))^2 + I(W\mathrm{cov}_{xy}(a,k))^2}$$

or

$$WR_{xy}(a,k) = \frac{\sqrt{R(W\mathrm{cov}_{xy}(a,k))^2 + I(W\mathrm{cov}_{xy}(a,k))^2}}{\sqrt{|W\mathrm{cov}_{xx}(a,0)|\,|W\mathrm{cov}_{yy}(a,0)|}}. \qquad (12)$$

In $WR_{xy}(a,\ k)$, the corresponding cross-correlation degree of time series $x(t)$ and $y(t)$ were quantitatively described for time scale (a) and time lag (k). To confirm the significance of the cross-correlation coefficient, a T-test was used for the test standards.

We drew an isogram of the wavelet cross-correlation coefficients and used it to quantitatively analyse the cross-correlation of different time series from whole to parts for a corresponding time scale and time lag for the purposes of integrated time-frequency analysis of the mutual relationship between the time sequences. Among them, both the maximum time scale and maximum time lag required 36 ten-day periods. We took into account the inter-annual cycle of vegetation, the basic cycle of which takes one year in the regions studied.

2.4 *Numerical analysis of the feedback effects of changes in vegetation on climate*

We used the method described by Liu *et al.* (2006) to conduct a numerical analysis of the feedback effects of changes in vegetation on climate. In general, the abnormal state variable of precipitation $P(t+dt)$ can be expressed as equation (13):

$$P(t+dt_a) = \lambda_A V(t) + N_a(t+dt_a), \qquad (13)$$

where $\lambda_A V(t)$ represents the atmospheric response to changes in vegetation $V(t)$ after time dt_a. The parameter λ_A represents the forcing efficiency, or feedback efficiency, of the vegetation on the atmosphere and will be referred to as the vegetation feedback parameter. $N_a(t\ +\ dt)$ represents the climate noise generated internally by the atmosphere independent of vegetation.

Multiplying equation (13) by $V(t-\tau)$, allows τ to represent the time lag. During analysis, the selection of time lag generally requires consideration of the correlation between early vegetation and vegetation at time t. The sample covariance (denoted by regular brackets [ ] in equation (14)) was calculated, and the noise tended towards zero because

atmospheric noise cannot affect early changes in vegetation,

$$[V(t-\tau),\ N_a(t+dt_a)] = 0, \quad \text{for } \tau > dt_a > 0.$$

$$\begin{aligned}&[V(t-\tau),\ P(t+dt_a)]\\ &= \lambda_A\,[V(t-\tau),\ V(t)] + [V(t-\tau),\ N_a(t+dt_a)]\end{aligned} \tag{14}$$

Considering that the response time of precipitation can be negligible when compared to the duration of the change in vegetation ($dt_a = 0$), we can use equation (15) to approximate the feedback coefficient of the vegetation on the precipitation.

$$\lambda_A = [V(t-\tau),\ P(t)]/[V(t-\tau), V(t)](dt \approx 0). \tag{15}$$

In theory, the estimator (equation 15) is independent of lag (as long as $\tau > 0$) because the changes with lag in the numerator and denominator cancel out. In practice, the sampling error of the estimator tends to increase with the lag because the diminishing denominator due to de-correlation tends to amplify the sampling error in the numerator. This is particularly true when the vegetation memory is not too much longer than the atmospheric memory. Therefore, it is best to use the estimation only for the first few lags. The sampling error also varies with the memory of the vegetation, with a longer vegetation memory giving a smaller sampling error.

To confirm the significance of vegetation feedback, a bootstrap approach with 1000 iterations, 95% of which were used for the test standards, was used to determine that the λ_A of the original sequence calculation was greater than the probability λ_A of the random sequence, which can reach a significance level of λ_A.

The variance percentage of vegetation feedback can be explained as equation (16):

$$\frac{\sigma^2\,[\lambda_A V(t)]}{\sigma^2\,[P(t)]}, \tag{16}$$

where $\sigma^2[\lambda_A V(t)]$ and $\sigma^2[P(t)]$ represent the variance of monthly precipitation owing to vegetative feedback and the total variance of monthly precipitation, respectively.

2.5 *Analysis of the response relationship between vegetation and precipitation and the tendencies of the vegetative feedback effect*

We obtained the feedback coefficient and wavelet cross-correlation coefficient for different time scales (a) and time lags (k) to characterize the cross-correlation of the different time series throughout the time domain and to indicate combinational information of size and distribution of cross-correlation (feedback factor) of the two time series on different time scales. We calculated the sum of wavelet cross-correlation (feedback coefficient) by integrating the corresponding two time series in the time lag (k) in the overall time domain by using equation (17):

$$WR_x(k) = \int WR_{xy}(a,k)^2\,da. \tag{17}$$

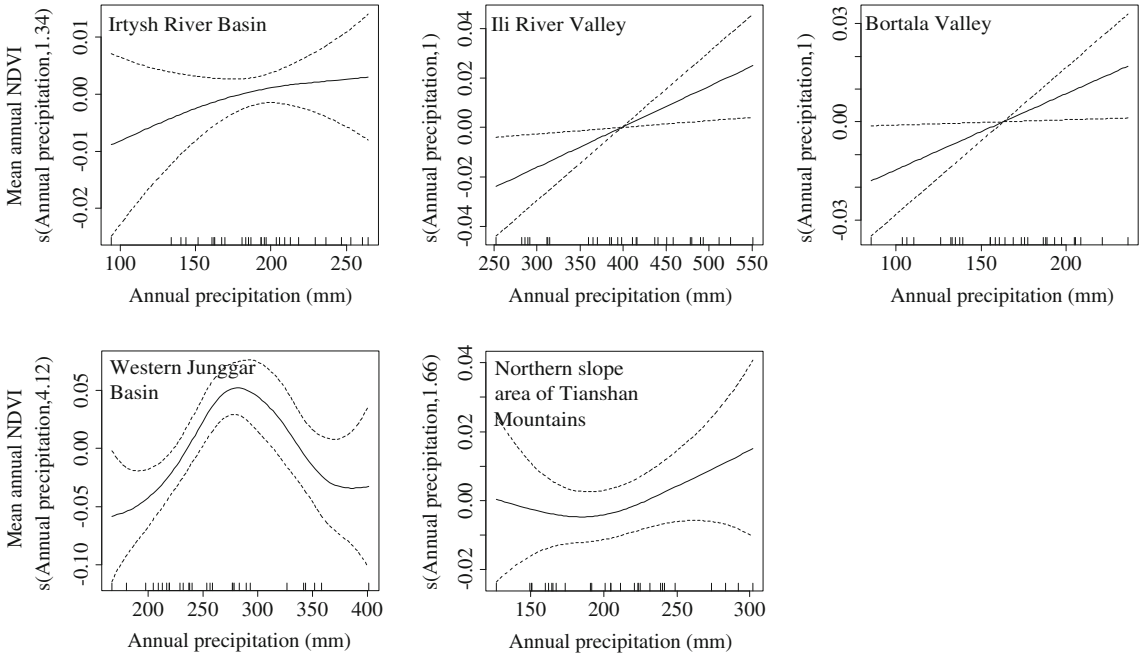

Figure 2. Mean annual NDVI *versus* relative annual precipitation (mm). Plots show partial effects of smooth trends based on linear regression models. All effects were significant for mean annual NDVI ($P < 0.05$). The short dashed lines (rugs) along the x-axis indicate annual precipitation. Changes in the annual precipitation and mean annual NDVI in the northern Tianshan Mountains (1981–2009).

Then the weight coefficients of the wavelet cross-correlation coefficient $WR_{xy}(a,k)$ (feedback coefficient λ_P) can be defined using equation (18):

$$f(WR_{xy}(a,k)) = \frac{WR_{xy}(a,k)^2}{WR_{xy}(k)}. \quad (18)$$

Then, the wavelet cross-correlation $WR(k)$ (degree of feedback $W\lambda(k)$) of two time series was defined using equation (19):

$$WR(k) = \int WR_{xy}(a,k) f(WR_{xy}(a,k))\, da, \quad (19)$$

where $WR(k)$ ($W\lambda(k)$) characterizes the degree of the cross-correlation (degree of feedback) of two time series with respect to time lag (k) throughout the time domain. The purpose of this characterization was to calculate the weighed expected values of the degree of cross-correlation (degree of feedback) of different time scales for the same time lag (k). The analysis of two time series in time scale (a) can be calculated using this method.

3. Results

3.1 *Interannual trend analysis of the precipitation and vegetation variation in the region*

In this paper, the Mann–Kendall test (Mann 1945; Kendall 1975) was used to characterize annual precipitation trends and mean annual NDVI trends.

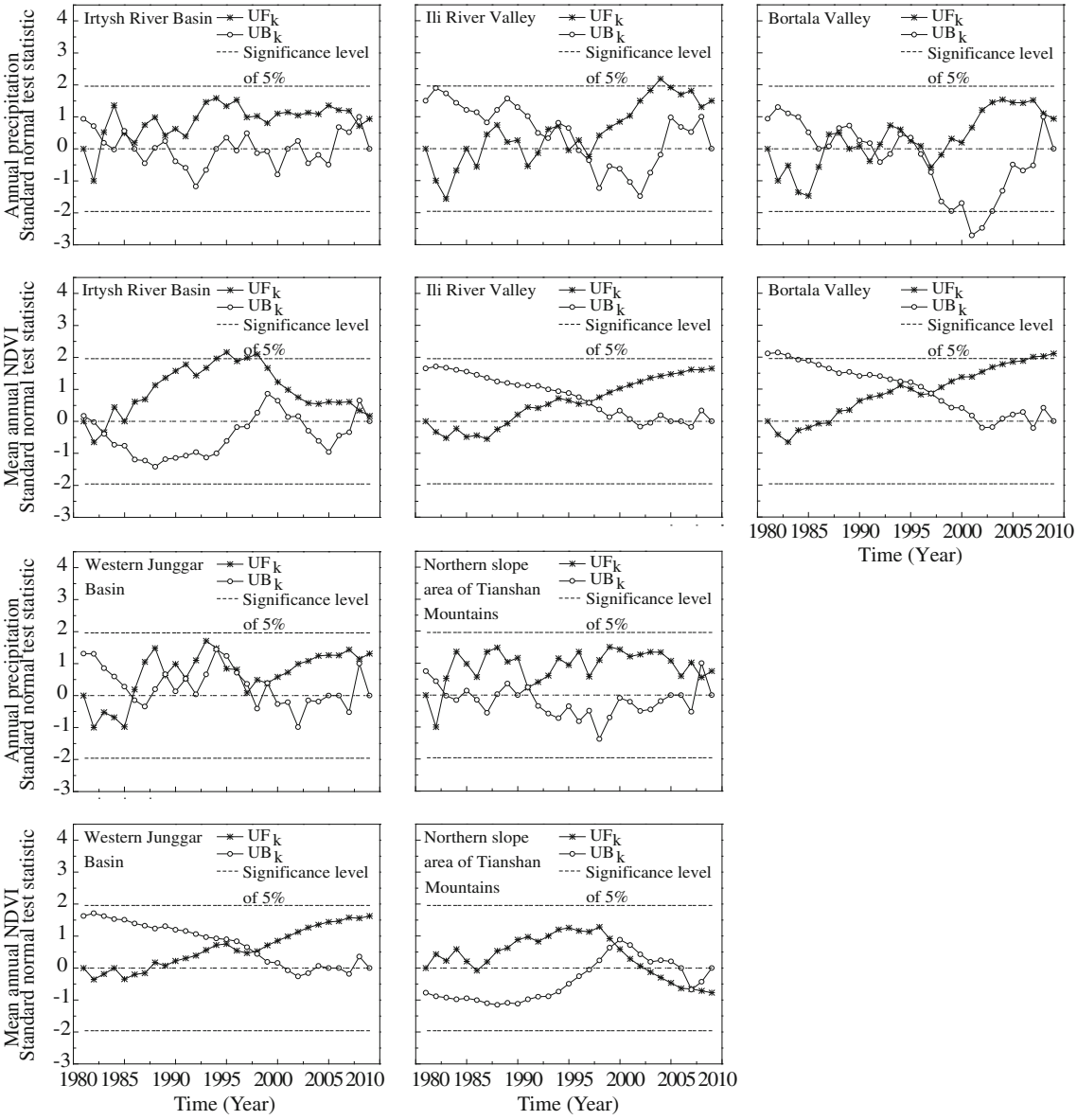

Figure 3. Mann–Kendall statistical curves of annual precipitation and mean annual NDVI in the northern Tianshan Mountains (1981–2009).

Mean annual NDVI varied with annual precipitation (figure 2). Annual precipitation over the past 30 years showed an increasing trend in the northern Tianshan Mountains (figure 3). The annual variation in NDVI was obviously distinct in the five regions evaluated in this study, showing an unconspicuous increasing trend in all regions except in the Irtysh River valley and the northern slopes of the Tianshan Mountains (figure 3). These values were compared to inter-annual changes in precipitation and vegetation, and vegetation showed a continuously increasing trend along with increasing precipitation observed in the Ili ($R^2 = 0.325$, $P < 0.05$) and Bortala ($R^2 = 0.415$, $P < 0.05$) valleys (figure 2).

3.2 *Analysis of the vegetative feedback effects on precipitation*

3.2.1 *Analysis of the wavelet cross-correlation coefficient isogram of the effects of feedback of changes in vegetation on precipitation*

In the northern Tianshan Mountains, the correlation between early changes in vegetation and subsequent precipitation has multiple time scale characteristics, and all regions showed similar overall correlations on different time scales (figure 4a). Significant differences were observed among the changes of the same time lag on different time scales. The positive and negative characteristics of cross-correlation in different time scales were not the same. Within any given time scale, the wavelet cross-correlation coefficient fluctuated with the time lag and gradually became very weak over time. The duration of each fluctuation, during which wavelet cross-correlation coefficient fluctuated with respect to the time lag, increased gradually as the time scale increased. When the time scale reached 30 ten-day periods ($a = 30$), cross-correlation showed an extreme centre when $k = 0$ and $k = 36$ ten-day periods (figure 4). When the time scale was 15 ten-day periods ($a = 15$), its extreme centre exists at time lag $k = 6$ ten-day periods. We amplified the regions for which the time scale $a \leq 15$ ten-day periods and time lag $k \leq 15$ ten-day periods (figure 4a). An extreme centre exists for which the time scale $a = 6$ ten-day periods and the time lag $k = 3$ or 9 ten-day periods (figure 4b).

When $a > 12$ ten-day periods, the similarity among the cross-correlations of the different regional time scales changed with respect to time lag and became more pronounced. In this case, it became difficult to analyse differences in the feedback effects of changes in vegetation on precipitation in different regions. However, when the time scale $a < 12$ ten-day periods, then the differences in these trends increased as the time scale decreased, showing that the correlation changed with respect

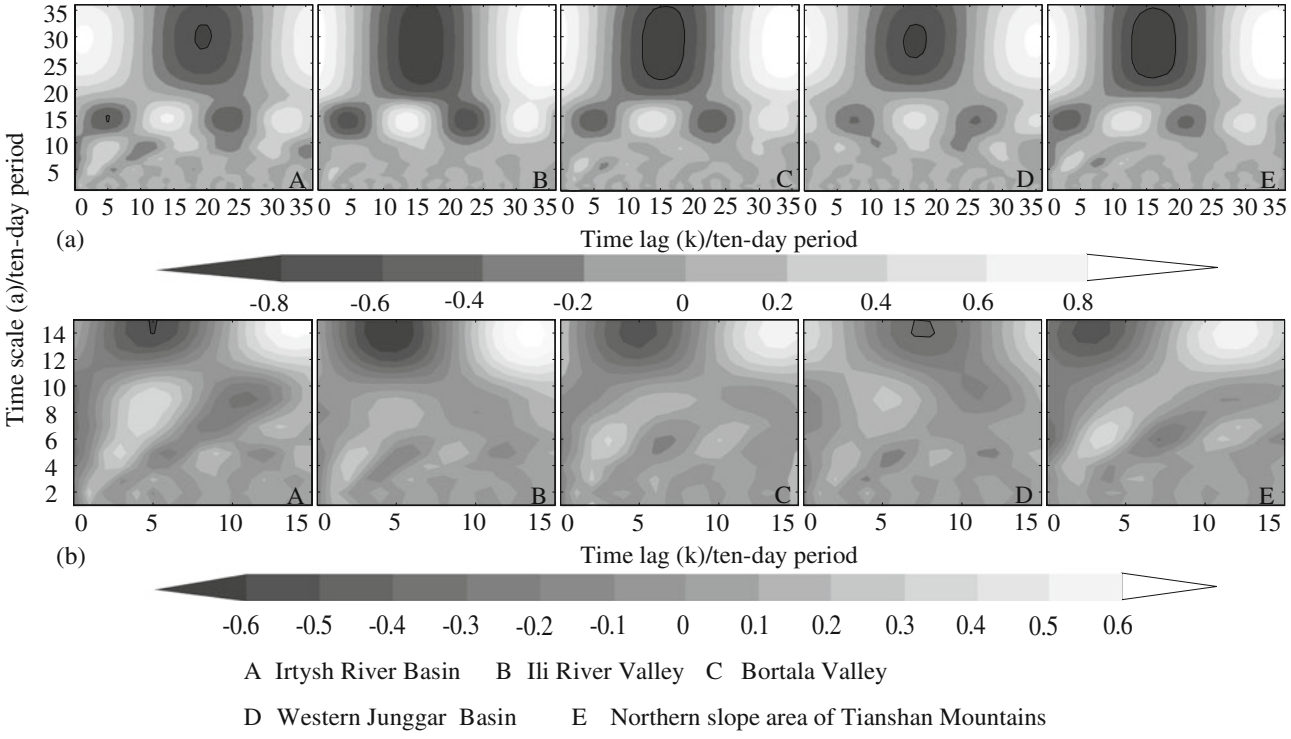

Figure 4. Wavelet cross-correlation coefficient isogram of NDVI and precipitation on a ten-day time scale (maximum time scales: (**a**) 36 ten-day periods and (**b**) 15 ten-day periods).

to time lag. The overall tendency of the regional correlation was similar in all parts of the northern Tianshan Mountains, although some obvious differences were observed (figure 4b). First, the time at which the extreme centre first emerged in each region varied, showing that the most obvious response relationship of precipitation to changes in vegetation occurred with respect to time scales. The tendency of the appearance of extreme points in the time lag phase was similar to that of the same time scale. However, the lag phase was different when the time scale differed among the regions, indicating that the speed of the response of precipitation to changes in vegetation differed across regions.

3.2.2 *Analysis of feedback effects of changes in vegetation on precipitation*

Figure 5 shows that (1) the explanation of vegetative feedback on changes in precipitation with a time scale that matches the time lag; (2) the time-scale most suitable to the analysis of the feedback effects of vegetation is different for different regions; (3) the feedback effect changes with the time scale and that a peak appears at 120–180 days, indicating that there is an optimal time scale (or time scale range) for the study of the effects of vegetative feedback on precipitation.

Figure 6 shows that (1) an explanation of the effects of vegetative feedback on changes in precipitation changes with the time lag within the same time scale, (2) the first peak in the changes within a half-year cycle (18 ten-day periods) appears at a time lag of 9–12 ten-day periods and the second appears at a time lag of 26–29 ten-day periods. Because the changes in precipitation and vegetation are cyclical, the first maximum is the time lag most suitable to analysis of vegetative feedback. Data collected after the time lag are affected by the cyclical nature of these changes and can conceal vegetative feedback. An optimal time lag scale (or range of time lag scales) can better indicate the effects of the vegetative feedback on precipitation, and (3) the lag phase of the effects of changes in vegetation on precipitation differs across regions.

4. Discussion

The analysis of 30-year trends in the changes in vegetation and precipitation in the northern Tianshan Mountains showed that precipitation is an important driving force behind these changes in vegetation. Although summarizing the effects of changes in vegetation on precipitation over time using a multi-year analysis of the regional trends is difficult, analysing the role of vegetation feedback using many time scales is necessary.

Studies have shown that changes in precipitation and vegetation in this region are cyclic and observable on multiple time scales. This may be the source of multiple time scale characteristics of the vegetation–precipitation relationship. Studies of the response relationship of precipitation on changes in vegetation have shown that the feedback effects of changes in vegetation on climate can differ significantly with different time lags. These studies have also verified the existence of these differences through a variety of numerical simulations (Liu *et al.* 2006; Notaro *et al.* 2008; Notaro and Liu 2008).

The effects of vegetation on precipitation involve positive feedback (Zhou and Wang 1999; Strengers *et al.* 2010). Transpiration decreases when vegetation cover is reduced, and this reduces convective cloud cover and rainfall. Reduced rainfall further reduces transpiration. When surface albedo increases, surface temperatures will drop, reducing transpiration and then rainfall (Bala *et al.* 2007). The loss of vegetation reduces rainfall by reducing surface roughness, surface transpiration, and sensible heat flux (Matthews *et al.* 2003). In addition, reduced vegetation cover results in increased levels of atmospheric CO_2, increased surface temperatures, and increased transpiration through the greenhouse effect. However, the increased concentration of CO_2 allows plants to obtain CO_2 from the atmosphere more easily. Plants respond by closing their stomata, with the ultimate effect appearing as a decline in vegetative transpiration (O'ishi *et al.* 2009; Li *et al.* 2013). The present study found that the effects of vegetation feedback on precipitation take place on multiple time scales. When the duration of each phase exceeds 12 ten-day periods, the regions tend to change in the same way. When the duration of each phase is less than 12 ten-day periods, the effects of vegetative feedback vary from region to region. Possible causes of these distribution characteristics are as follows: First, the scale used in this study to evaluate these effects may have been too large. The use of smaller units of time may show the effects better. The feedback effects of changes in vegetation on later precipitation are dispersed. The large units of time used here to evaluate changes in the periodic variations in vegetation and the multiple time scale characteristics of precipitation may have affected the results of the study. This occurred because the multiple time scale characteristics of the vegetative feedback effect are similar to the periodic changes in the vegetation at time scales of 36 ten-day periods. Second, the differences among the various regions of the northern Tianshan Mountains within any given climate context and regional moisture source are

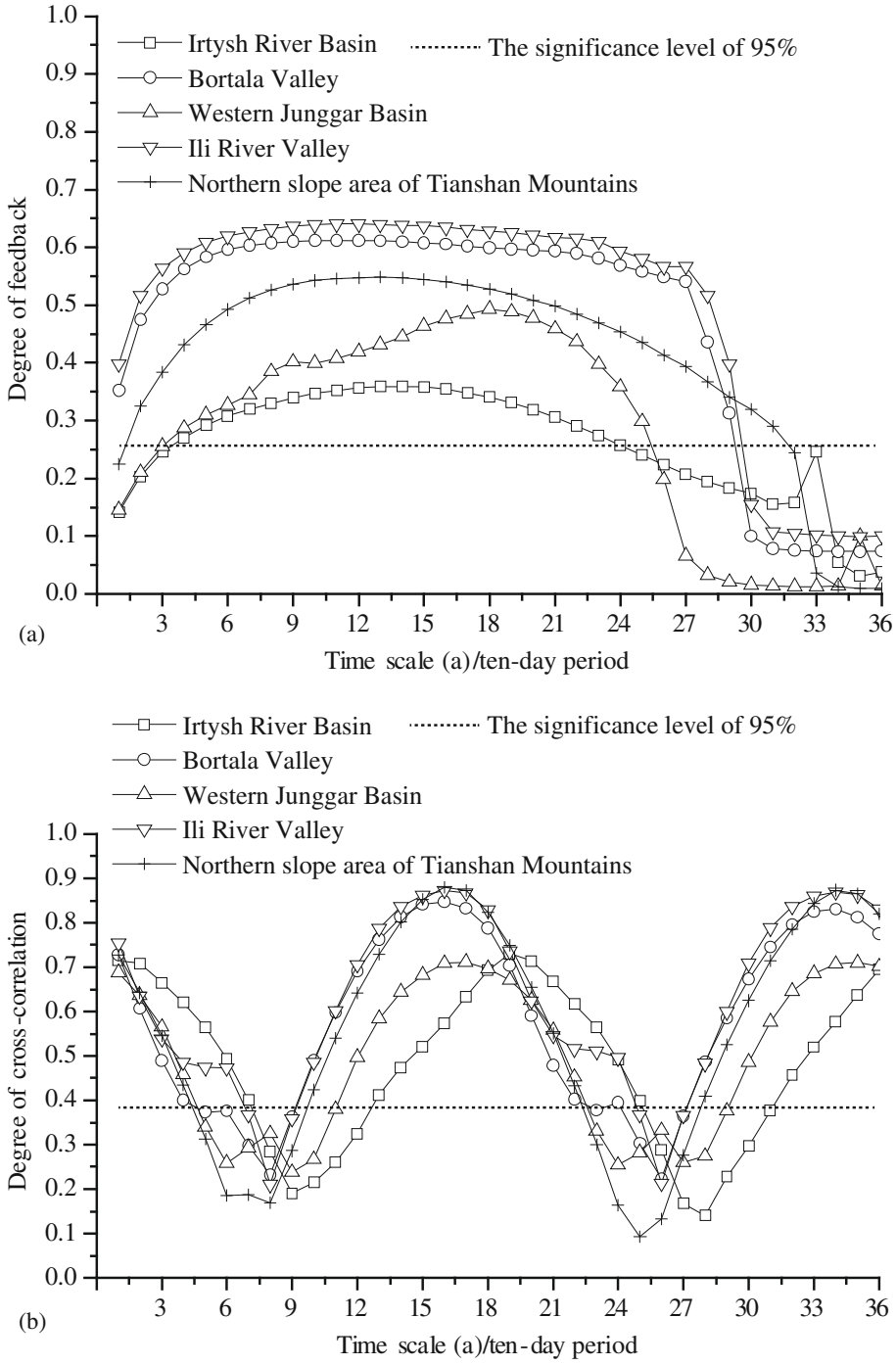

Figure 5. (**a**) Results of numerical calculation explaining the effects of vegetative feedback on changes in precipitation with a time lag that matches the time scale. (**b**) Results of wavelet cross correlation showing patterns of the cross correlation of time scale to precipitation.

very small. Third, in winter, precipitation comes mainly in the form of snowfall in this cold and arid region, vegetation is sparse, and the NDVI value approaches zero, which also affects the vegetation feedback effects. When the time scales are less than 12 ten-day periods, it appears that the differences of precipitation among regions must be evaluated using smaller units of time, which may ignore the effects of different forms of precipitation observed in each region. This issue merits further study.

The results of the study on the response relationship during the study period were consistent with those of previous studies on feedback effects (Zhang *et al.* 2003; Liu *et al.* 2006; Hua *et al.* 2008; Mao *et al.* 2008; Wang *et al.* 2010; Zuo *et al.* 2010). The effects

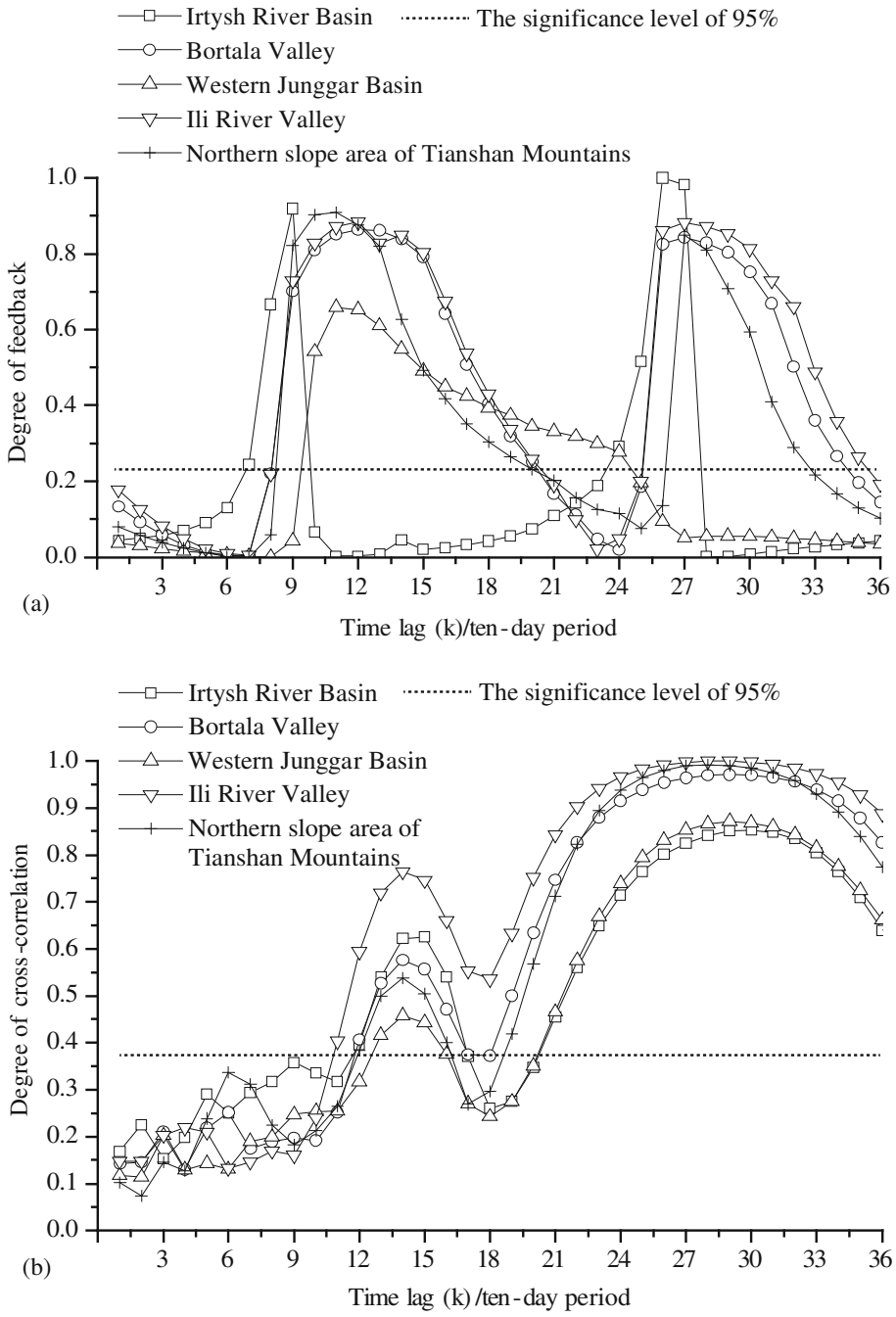

Figure 6. (**a**) Results of numerical calculation explaining the effects of vegetative feedback on changes in precipitation with a time scale that matches the time lag. (**b**) Wavelet cross correlation showing patterns of the cross correlation of time scale to precipitation.

of vegetative feedback on precipitation were found to involve multiple time scales. Although, the conclusions of the wavelet cross-correlation analysis were the same as the results of the correlation analysis between the early changes in vegetation and later precipitation, the cross-correlation analysis included not only the feedback effects of the early changes in vegetation on later precipitation but also the effect of changes in change on vegetation. In this way, the wavelet cross-correlation analysis indicated a correlation exists between changes in vegetation and precipitation on different scales of analysis and with different time delay correlations. In contrast, numerical calculations of the vegetative feedback primarily analyse the feedback effects of changes in vegetation on later precipitation. Although the method involves only one time scale, this method has been proven very accurate in the analysis of feedback effects of changes in vegetation on precipitation.

5. Conclusion

The analysis of 30-year trends in the changes in vegetation and precipitation in the northern Tianshan Mountains showed vegetation and precipitation have the same tendencies everywhere in the study region except on the northern slopes of the Tianshan Mountains. It also showed that precipitation is an important driving force behind these changes in vegetation. Numerical analysis of feedback information from vegetation, combining WA and cross-correlation techniques, was used to study the feedback effect of the changes in vegetation on precipitation on different time scales and time lags. The effects of feedback appeared to vary in these five regions when different time scales were used to examine them. The most useful time scale was generally found to be 4–6 months. Time lag was another characteristic of this process, and the optimal time lag was 3–4 months. Nevertheless, the optimal time scale and time lag did not differ significantly in these five regions. The present study showed that the wavelet cross-correlation analysis is specific and superior to an analysis using multiple time scales. It can provide a reference for numerical calculations of vegetative feedback. In this way, wavelet cross-correlation analysis can specify the distinct time scales and time lags of the effects of changes in vegetation on the precipitation. This facilitates identification of the optimal time scale and time lag of vegetation feedback using numerical analysis.

Acknowledgements

The research presented in this paper is funded by the National Science Foundation of China (31260099); Key Technology R & D Program (2014BAC14B02); National Natural Science Foundation of China (41375079); National Key Basic Research Program of China (2013CB430204); and Major National Scientific Research Programs of China (2012CB955902).

References

Alo C A and Wang G 2010 Role of dynamic vegetation in regional climate predictions over western Africa; *Clim. Dyn.* **35** 907–922.

Bala G, Caldeira K, Wickett M, Phillips T, Lobell D, Delire C and Mirin A 2007 Combined climate and carbon-cycle effects of large-scale deforestation; *Proc. Nat. Acad. Sci.* **104** 6550.

Brovkin V, Claussen M, Driesschaert E, Fichefet T, Kicklighter D, Loutre M F, Matthews H D, Ramankutty N, Schaeffer M and Sokolov A 2006 Biogeophysical effects of historical land cover changes simulated by six earth system models of intermediate complexity; *Clim. Dyn.* **26** 587–600.

Brunsell N 2010 A multiscale information theory approach to assess spatial-temporal variability of daily precipitation; *J. Hydrol.* **385** 165–172.

Davin E L and De Noblet-Ducoudré N 2010 Climatic impact of global-scale deforestation: Radiative *versus* nonradiative processes; *J. Climate* **23** 97–112.

Gao W and Li B 1993 Wavelet analysis of coherent structures at the atmosphere–forest interface; *J. Appl. Meteorol.* **32** 1717–1725.

Goetz S J, Fiske G J and Bunn A G 2006 Using satellite time-series data sets to analyze fire disturbance and forest recovery across Canada; *Remote Sens. Environ.* **101** 352–365.

Holben B N 1986 Characteristics of maximum-value composite images from temporal AVHRR data; *Int. J. Remote Sens.* **7** 1417–1434.

Hua W, Fan G, Zhou D, Ni C, Li X, Wang Y, Liu Y and Huang X 2008 Preliminary analysis on the relationships between Tibetan Plateau NDVI change and its surface heat source and precipitation of China; *Science in China Series D: Earth Sci.* **51** 677–685.

Hudson I, Keatley M and Kang I 2011 Wavelet characterization of eucalypt flowering and the influence of climate; *Environ. Ecolog. Stat.* **18** 513–533.

Kaptué Tchuenté A T, De Jong S M, Roujean J L, Favier C and Mering C 2011 Ecosystem mapping at the African continent scale using a hybrid clustering approach based on 1-km resolution multi-annual data from SPOT/VEGETATION; *Remote Sens. Environ.* **115** 452–464.

Kendall M G 1975 Rank correlation methods; Griffin, London, UK.

Kisi O 2011 Wavelet regression model as an alternative to neural networks for river stage forecasting; *Water Resour. Manag.* **25** 579–600.

Li W, Ji J, Dong W and Liu X 2008 Diagnosis of global vegetation–atmosphere interactions at the interannual time scale; *Chinese J. Atmos. Sci.* **32** 75–89.

Li B 2000 Fractal geometry applications in description and analysis of patch patterns and patch dynamics; *Ecol. Modelling* **132** 33–50.

Li B and Loehle C 1995 Wavelet analysis of multiscale permeabilities in the subsurface; *Geophys. Res. Lett.* **22** 3123–3126.

Li C, Zhang C, Luo G and Chen X 2013 Modelling the carbon dynamics of the dryland ecosystems in Xinjiang, spatiotemporal patterns and climate controls; *Ecol. Modelling* **267** 148–157.

Liu Z, Notaro M, Kutzbach J and Liu N 2006 Assessing global vegetation–climate feedbacks from observations; *J. Climate* **19** 787–814.

Mann H B 1945 Nonparametric tests against trend; *Econometrica* **13** 245–259.

Mao R, Gong D and Fang Q 2008 Possible impacts of vegetation cover on local meteorological factors in growing season; *Clim. Environ. Res.* **13** 738–750.

Matthews H D, Weaver A J, Eby M and Meissner K J 2003 Radiative forcing of climate by historical land cover change; *Geophys. Res. Lett.* **30** 1055.

Notaro M and Liu Z 2008 Statistical and dynamical assessment of vegetation feedbacks on climate over the boreal forest; *Clim. Dyn.* **31** 691–712.

Notaro M, Wang Y, Liu Z, Gallimore R and Levis S 2008 Combined statistical and dynamical assessment of simulated vegetation–rainfall interactions in North Africa during the mid-Holocene 1; *Global Change Biology* **14** 347–368.

O'ishi R, Abe-Ouchi A, Prentice I C and Sitch S 2009 Vegetation dynamics and plant CO_2 responses as positive feedbacks in a greenhouse world; *Geophys. Res. Lett.* **36** L11706.

Paeth H, Born K, Girmes R, Podzun R and Jacob D 2009 Regional climate change in tropical and northern Africa due to greenhouse forcing and land use changes; *J. Climate* **22** 114–132.

Paluš M, Novotná D and Tichavský P 2005 Shifts of seasons at the European mid-latitudes: Natural fluctuations correlated with the North Atlantic Oscillation; *Geophys. Res. Lett.* **32** L12805.

Pitman A, de Noblet-Ducoudré N, Cruz F, Davin E, Bonan G, Brovkin V, Claussen M, Delire C, Ganzeveld L and Gayler V 2009 Uncertainties in climate responses to past land cover change: First results from the LUCID intercomparison study; *Geophys. Res. Lett.* **36** L14814.

Rehman S and Siddiqi A 2009 Wavelet based correlation coefficient of time series of Saudi Meteorological Data; *Chaos, Solitons & Fractals* **39** 1764–1789.

Sang Y, Wang D, Wu J and Zhu Q 2010 Wavelet cross-correlation method for hydrologic time series analysis; *J. Hydraul. Eng.* **41** 1272–1279.

Shi Y, Shen Y and Hu R 2002 Preliminary study signal, impact and foreground of climatic shift from warm-dry to warm-humid in northwest China; *J. Glaciol. Geocryol.* **24** 219–226.

Stow D, Petersen A, Hope A, Engstrom R and Coulter L 2007 Greenness trends of Arctic tundra vegetation in the 1990s: Comparison of two NDVI data sets from NOAA AVHRR systems; *Int. J. Remote Sens.* **28** 4807–4822.

Strengers B J, Müller C, Schaeffer M, Haarsma R J, Severijns C, Gerten D, Schaphoff S, van den Houdt R and Oostenrijk R 2010 Assessing 20th century climate–vegetation feedbacks of land-use change and natural vegetation dynamics in a fully coupled vegetation–climate model; *Int. J. Climatol.* **30** 2055–2065.

Wang W, Jin J and Li Y 2009 Prediction of inflow at three gorges dam in Yangtze River with wavelet network model; *Water Resour. Manag.* **23** 2791–2803.

Wang W, Hu S and Li Y 2011 Wavelet transform method for synthetic generation of daily streamflow; *Water Resour. Manag.* **25** 41–57.

Wang Y, Zhao P, Yu R and Rasul G 2010 Inter-decadal variability of Tibetan spring vegetation and its associations with eastern China spring rainfall; *Int. J. Climatol.* **30** 856–865.

Wu L, Zhang J and Dong W 2011 Vegetation effects on mean daily maximum and minimum surface air temperatures over China; *Chinese Sci. Bull.* **56** 900–905.

Xie J and Liu T 2010 Characterization of spatial scaling relationships between vegetation pattern and topography at different directions in Gurbantunggut desert, China; *Ecological Complexity* **7** 234–242.

Zeng N 2003 Atmospheric science. Drought in the Sahel; *Science* **302** 999–1000.

Zhang J and Deng Z 1987 Introduction of Xinjiang precipitation; Beijing, China Meteorological Press.

Zhang J, Dong W and Ye D 2003 New evidence for effects of land cover in China on summer climate; *Chinese Sci. Bull.* **48** 401–405.

Zhang X 2001 Ecological restoration and sustainable agricultural paradigm of Mountain Oasis Ecotone Desert system in the north of the Tianshan Mountains; *Acta Botanica Sinica* **43** 1294–1299.

Zhang C, Li C, Luo G and Chen X 2013 Modeling plant structure and its impacts on carbon and water cycles of the central Asian arid ecosystem in the context of climate change; *Ecol. Modelling* **267** 158–179.

Zhang G, Xu X, Zhou C, Zhang H and Ouyang H 2011 Responses of grassland vegetation to climatic variations on different temporal scales in Hulun Buir Grassland in the past 30 years; *J. Geogr. Sci.* **21** 634–650.

Zhou G and Wang Y 1999 The feedback of land use/cover change on climate; *J. Nat. Resources* **4** 318–322.

Zuo Z, Zhang R and Zhao P 2010 The relation of vegetation over the Tibetan Plateau to rainfall in China during the boreal summer; *Clim. Dyn.* **36** 1207–1219.

MS received 30 June 2015; revised 24 November 2015; accepted 30 November 2015